PREPRINT: Atmospheric CO2 source analysis

Tom Quirk* and Michael Asten

Quirk affiliation

michael.asten.monash@gmail.com (MA)

* Correspondence: twquirk@labyrinth.net.au

Abstract: This analysis uses both atmospheric CO2 concentrations and the accompanying $\delta^{13}C$ isotopic measurements of CO2 for 40 years from 1978 to 2017. Atmospheric CO2 has been separated into two components of CO2 coming from ocean and plant sources. The isotopic values given to the components are $\delta\,^{13}C = 0\ ‰$ for the ocean-component and -26 ‰ for the plant component.

The latitude variations in component CO2 show the ocean component peaking at the equator. This contrasts with the plant component which peaks in the Arctic Circle region. Seasonal summer-winter comparisons show no change in the ocean component peaking at the equator and no significant changes in magnitude while there are substantial changes in the plant component.

The ocean and plant components of atmospheric CO2 are independent sources of atmospheric CO2 with approximately equal at 50%.

Keywords: ocean CO2, atmospheric CO2, $\delta\,^{13}C$ isotope

1. Introduction

The prediction of future global temperatures by computer models depends on the prediction of the future levels of CO2 in the atmosphere. This in turn depends on understanding and predicting the variability of exchanges from sources and sinks of CO2 often referred to as the Global Carbon Cycle [1].

The Global Carbon Cycle models the interactions of the atmosphere with the oceans and the biosphere. Much of this model analysis predates the measurements of the isotopic composition of atmospheric CO2 commencing in the early 1980s. In fact, there are now some 40 years of atmospheric concentrations and $\delta^{13}C$ isotope composition measurements of CO2 available from the Scripps Institution of Oceanography [2] (SIO) commencing in 1978. The SIO stations and years with both CO2 and $\delta^{13}C$ measurements are listed in Table 1.

Table 1: SIO year for CO2 and $\delta^{13}C$ measurements.

	Latitude	**Longitude**	**Elevation (metres)**	**Years with CO2 and $\delta^{13}C$**
Alert	82 N	63 W	210	1986 - 2018
Point Barrow	71 N	157 W	11	1983 - 2018
La Jolla	33 N	117 W	10	1979 - 2018
Kumukahi	19 N	155 W	3	1981 - 2018
Mauna Loa	19 N	156 W	3,397	1981 - 2018
Christmas Island*****	2 N	157 W	2	1978 - 2018
American Samoa	14 S	171 W	30	1985 - 2018
Kermadec	29 S	178 W	2	1985 - 2015
Baring Head	41 S	175 E	85	1986 - 2018
South Pole	90 S		2,810	1978 - 2018

*****Note that Christmas Island is part of the Republic of Kiribati in the Pacific Ocean.

The apparent smooth and continuous rise in atmospheric CO2 concentrations has been shown to be broken into a series of changing trends associated with ocean decadal phase changes [3]. The following analysis expands on the earlier paper by using both atmospheric CO2 concentrations and the accompanying isotopic measurements of carbon in the CO2.

The measure of the ratio of C12 to C13 found in a sample of CO2 is expressed as $\delta^{13}C$, where C13 / C12 are of order 0.01. Variations of $\delta^{13}C$ are attributable to variations in the molecular weight of CO2 which affect

the rate of chemical reactions and photosynthesis. $\delta^{13}C$ is expressed as the difference from a standard carbon source in tenths of a percent (‰).

This analysis uses the CO2 concentration and isotope measurements after 1978 to divide the atmospheric CO2 concentration into an "ocean" and a "plant" component by assuming values for the isotopic composition for the two components.

2. Ocean and Plant contributions to atmospheric CO2

The basis of this analysis is the assumption that ocean and plant contributions to atmospheric CO2 are independent and may each act as a source and/or a sink of atmospheric CO2.

The separation of ocean and plant contributions can be quantified using the two relations defined in equations 1 and 2:

$$A_{meas} = A_{ocean} + A_{plant} \quad (1)$$

$$\delta^{13}C_{meas} = (\delta^{13}C_{ocean} \times A_{ocean} + \delta^{13}C_{plant} \times A_{plant}) / A_{meas} \quad (2)$$

where

A_{meas} is the measured atmospheric concentration of CO2 in ppm

A_{ocean} is the component of ocean origin, in ppm,

A_{plant} is the component of plant origin, in ppm,

$\delta^{13}C_{meas}$ is the isotopic value of measured atmospheric CO2,

$\delta^{13}C_{ocean}$ is the isotopic value of "ocean" component atmospheric CO2, and

$\delta^{13}C_{plant}$ is the isotopic value of "plant" component atmospheric CO2.

So, the separate components calculated using the measured values for the atmospheric CO2, and assuming isotopic values for "ocean" and "plant" components, are given by equations 3 and 4

$$A_{ocean} = A_{meas} \times (\delta^{13}C_{meas} - \delta^{13}C_{plant}) / (\delta^{13}C_{ocean} - \delta^{13}C_{plant}) \quad (3)$$

$$A_{plant} = A_{meas} - A_{ocean} \quad (4)$$

Measured atmospheric concentrations are recorded in parts per million (ppm) by volume. Thus, to separate an ocean and a plant source component requires converting ppm by volume to ppm by mass. However, the correction is less than 0.001 ppm where measuring errors are 0.1 ppm. So, the concentration value need not be corrected.

For this analysis

- $\delta^{13}C_{ocean} = 0$ ‰ from deep ocean measurements [4]; a summary [5] of these measurements range from 0 to +1 ‰. A value of $\delta^{13}C_{ocean} = +1$ ‰ is used in modeling the carbon cycle in [6].
- $\delta^{13}C_{plant} = -26$ ‰ for plants, applicable to C3 plants [7], phytoplankton species for north and south high latitudes [8], and fossil fuels [9].

The range of measured values compared to the chosen values is considered in Section 5 by varying the chosen values of $\delta^{13}C$ by ± 2 ‰.

3. Ocean and plant component contributions from monthly measurements

The monthly measurements for the South Pole and Christmas Island from 1978 to 2018 and Point Barrow from 1980` to 2018 are shown in Figure 1. The ocean and plant source components of atmospheric CO2 have been computed using equations 3 and 4. The results from the monthly measurements of atmospheric CO2 concentrations and $\delta^{13}C$ are shown in Figures 2, and 3 for the South Pole and Christmas Island from 1978 to 2018 and Point Barrow from 1983` to 2018.

The seasonal variations seen in the measured CO2 concentrations are found in the plant component but not to any significant extent in the ocean component.

Further the ocean component for Christmas Island has the highest values and Point Barrow and the South Pole the lowest values as seen in Figure 2 while the total CO2 concentration (Figure 1) and the plant component (Figure 3) show Point Barrow with the highest value and the South Pole with the lowest values.

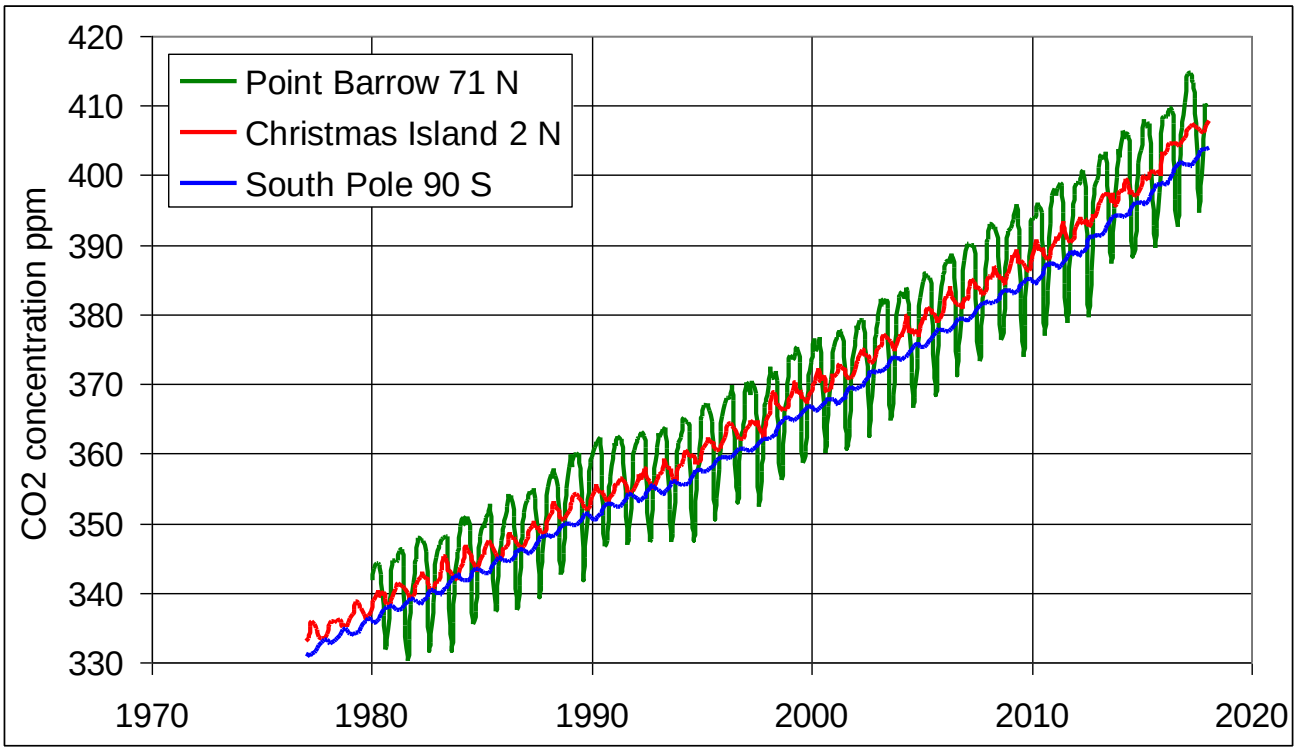

Figure 1. Monthly atmospheric CO2 concentrations at the South Pole, 90 S, Christmas Island, 2 N and Point Barrow, 71 N for 1978 to 2018.

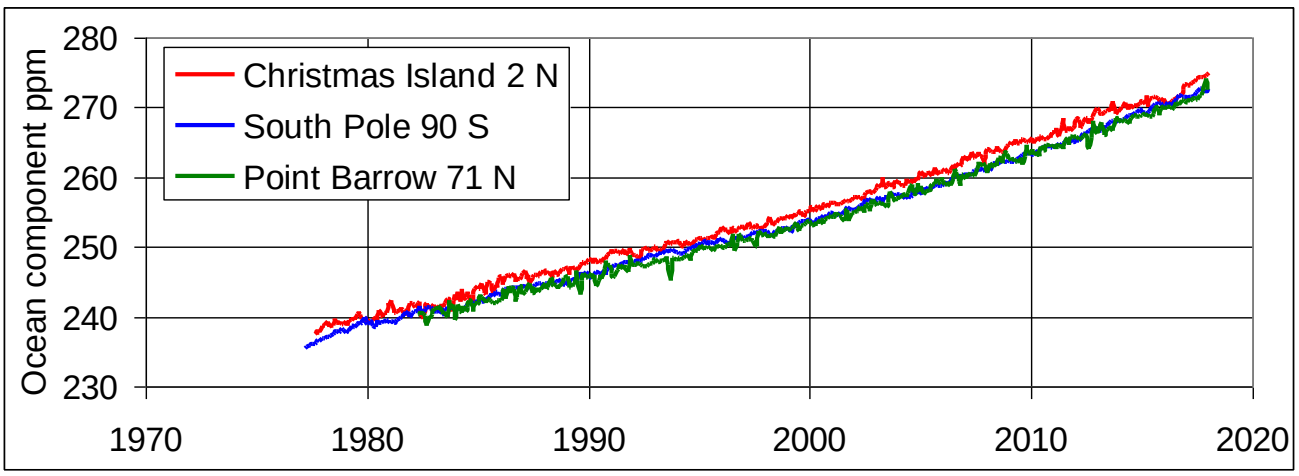

Figure 2. Monthly ocean component CO2 concentrations at the South Pole,90,S, Christmas Island, 2 N and Point Barrow, 71 N for 1978 to 2018.

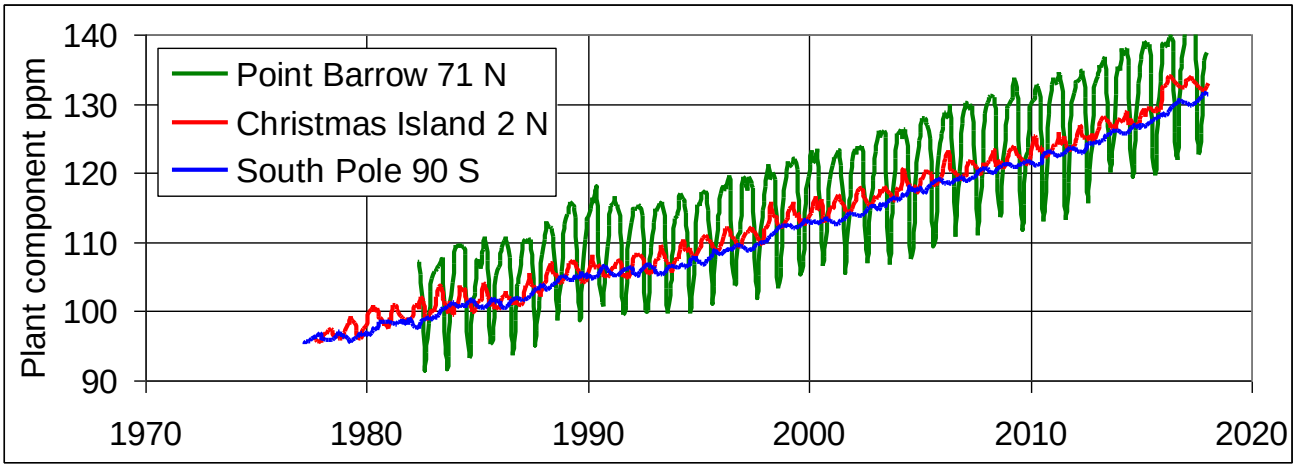

Figure 3. Monthly plant component CO2 concentrations at the South Pole 90 S, Christmas Island, 2 N and Point Barrow, 71 N for 1978 to 2018.

In the following discussion we focus on the time interval 1986 to 2015 since this is the period where measured data is available for a maximum range of latitudes (next section). The annual increases from 1986 to 2015 have been found by a least-squares fit to the three curves shown in Figure 3 and these are listed in Table 2. The most remarkable result is that the ocean and plant annual increases are similar.

Table 2. Annual CO2 increases from 1986 to 2015 from monthly data.

	Annual increases in ppm		
Stations	**CO2 concentration**	**Ocean component**	**Plant component**
South Pole 90 S	1.77	0.89	0.88
Christmas Island 2 N	1.81	0.90	0.91
Point Barrow 71 N	1.80	0.90	0.90

The behavior of the ocean and plant components will be further explored by analysis of all SIO latitudes annual measurements.

4. Ocean and plant source component latitude analysis for annual values

We consider variation of residual atmospheric CO2 measurements as measured at the ten SIO stations listed in Table 3, where the residual is the measured value less the value at the South Pole averaged over 1986 to 2015. This is the period where there are concentration and isotopic composition CO2 measurements for all latitudes.

Figure 4 shows the annual latitude variations of residual CO2, and it is apparent that the variation of atmospheric CO2 measurements shows increasing concentrations from the lowest values at the South Pole 90˚ S to a peak at Point Barrow 71˚ N.

Table 3. Residual ocean component values for 1986 to 2015. Highlighted values show the perturbation attributable the effect of altitude at Mauna Loa.

SIO Stations	Latitude	Longitude	Elevation (metres)	Residual values from South Pole value in ppm		
				Mean	Standard deviation	Error of mean
Alert	82 N	63 W	210	-0.29	0.31	0.06
Point Barrow	71 N	157 W	11	-0.35	0.38	0.07
La Jolla	33 N	117 W	10	0.36	0.40	0.07
Kumukahi	**19 N**	**155 W**	**3**	**0.70**	**0.39**	**0.07**
Mauna Loa	**19 N**	**156 W**	**3,397**	**0.99**	**0.24**	**0.04**
Christmas Island	2 N	157 W	2	1.60	0.39	0.07
American Samoa	14 S	171 W	30	0.94	0.26	0.05
Kermadec	29 S	178 W	2	0.38	0.31	0.06
Baring Head	41 S	175 E	85	0.16	0.27	0.05
South Pole	90 S		2,810	0.00		

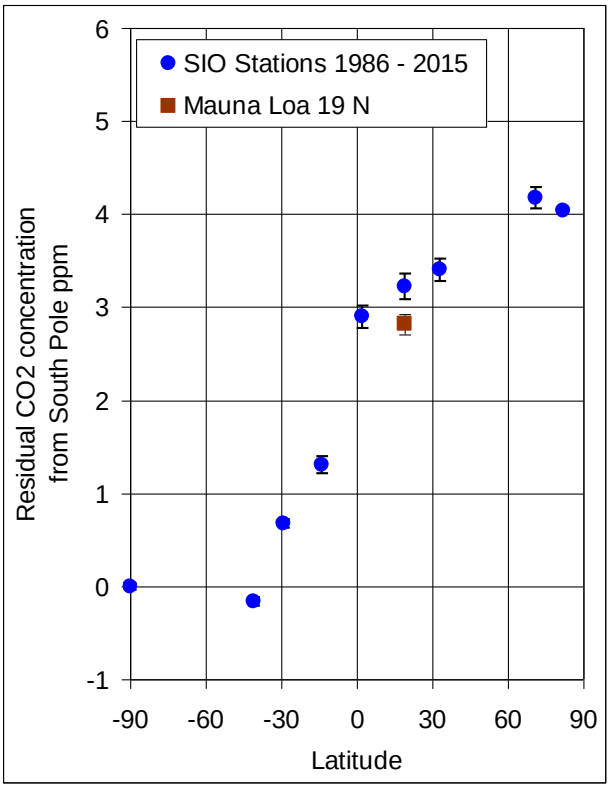

Figure 4. Annual latitude variations of atmospheric CO2 less the value at the South Pole averaged for SIO measurements.

Table 4. Residual plant component values for 1986 to 2015.

SIO Stations	Latitude	Longitude	Elevation (metres)	Residual values from South Pole value in ppm		
				Mean	Standard deviation	Error of mean
Alert	82 N	63 W	210	4.33	0.57	0.10
Point Barrow	71 N	157 W	11	4.52	0.58	0.11
La Jolla	33 N	117 W	10	3.04	0.74	0.14
Kumukahi	**19 N**	**155 W**	**3**	**2.52**	**0.52**	**0.09**
Mauna Loa	**19 N**	**156 W**	**3,397**	**1.83**	**0.59**	**0.10**
Christmas Island	2 N	157 W	2	1.30	0.47	0.09
American Samoa	14 S	171 W	30	0.37	0.30	0.05
Kermadec	29 S	178 W	2	0.30	0.31	0.06

Baring Head	41 S	175 E	85	-0.32	0.24	0.04
South Pole	90 S		2,810	0.00		

The latitude variations of the CO2 concentrations are quite different when separated into ocean and plant components. The component values, standard deviations and errors of the mean are listed in Tables 3 and 4 and plotted in Figure 5. The ocean component is at a maximum near the equator (Figure 5a) in contrast with the plant component which shows a maximum above the Arctic Circle at latitudes of Point Barrow 71˚ N and Alert 82˚ N (Figure 5b).

The analysis also shows significantly different residual values at Mauna Loa at an elevation of 3397 m compared to Kumukahi at 3 m (highlighted in Tables 3 and 4). The ocean component residual at Mauna Loa is significantly greater than the Kumukahi residual while this is reversed with the Mauna Loa plant component residual being significantly less than the Kumukahi residual. These differences are shown in Figure 5.

We make the hypothesis that the differences may be due to the elevation at which Mauna Loa measurements are made above the sub-tropical inversion so the atmosphere is more mixed with contributions from the equatorial region adding higher residual ocean component to that found at Kumukahi at 3 m. Likewise, the plant component values in the equatorial region are less than that at Kumukahi so the Mauna Loa plant residual is mixed to a lower value than the Kumukahi residual plant value.

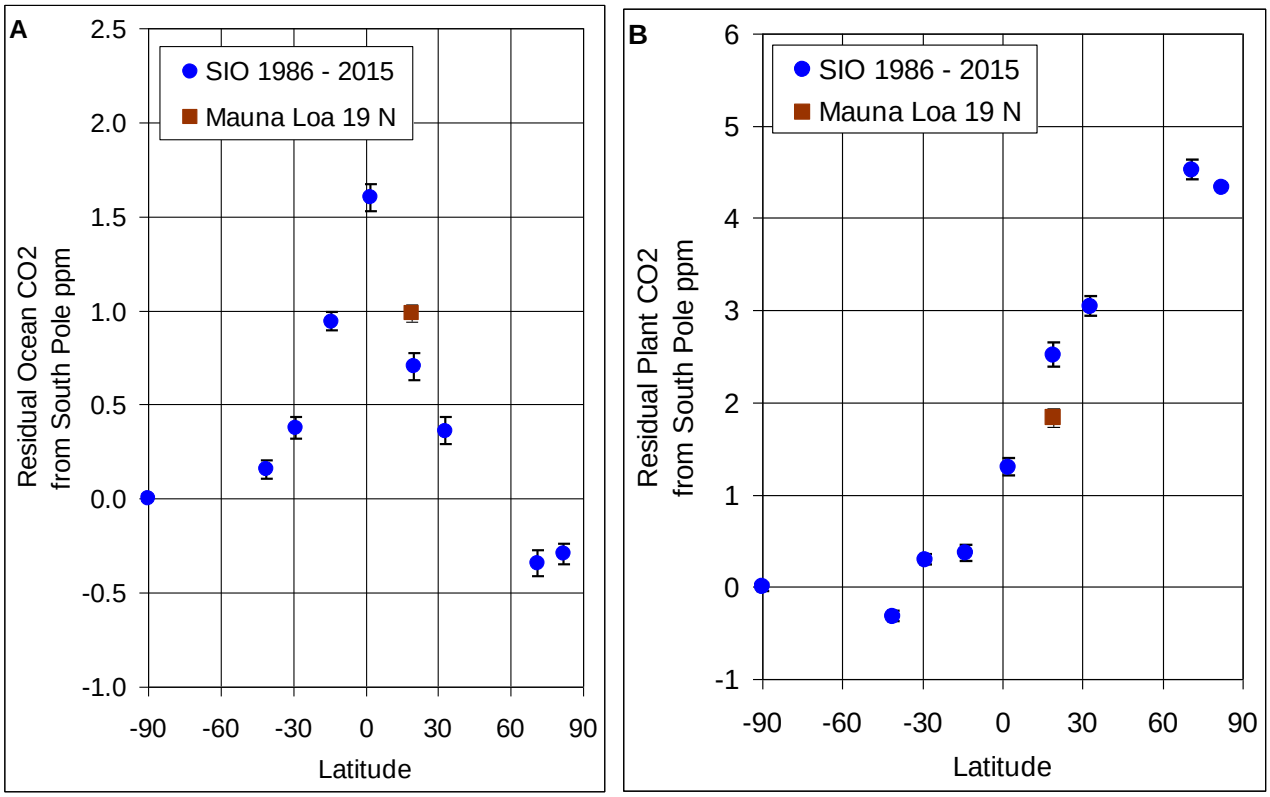

Figure 5. Latitude variations of CO2 source components less the value at the South Pole from SIO for (a) the ocean component and (b) the plant component.

The differing latitude dependence of the ocean component and the plant components suggests the two are driven by different mechanisms.

If the ocean source component is independent of the plant source component then the ocean source peaking at the equator should be independent of seasonal variations

Figures 6 and 7 show seasonal separations for the months of February to March and of August to September, for the ocean and plant components of CO2 for all latitudes. There is little change in the ocean components for the seasonally separated values relative to the annual average residuals. The stability of the ocean source CO2 can be seen by comparing the latitude seasonal changes for February and March with those of August and September (Figures 6a, 7a) and by plotting the numerical seasonal differences in Figure 8. This latter plot shows that seasonal differences for ocean source values are not statistically different with the exception of Christmas Island 2 N, American Samoa 14 S and Kermadec Island 29 S. This is due to the mixing of CO2 from the northern hemisphere to the southern hemisphere during the winter months. However in the northern summer there is no mixing from south to north.

The latitude and seasonal variations in the plant component are quite different. The plant component shows deviations of up to 15 ppm from summer to winter at the far-north sites of Point Barrow and Alert (Figures 6b, 7b).

The hypothesis for this seasonal difference is that plant variations in the Northern Hemisphere are dominantly due to the boreal forests that are north of latitude 30 ºN. The trees start to grow in Spring drawing CO2 from the atmosphere while at the end of Summer growth reduces the draw-down of CO2. In addition, it is expected that decaying plants will return CO2 to the atmosphere.

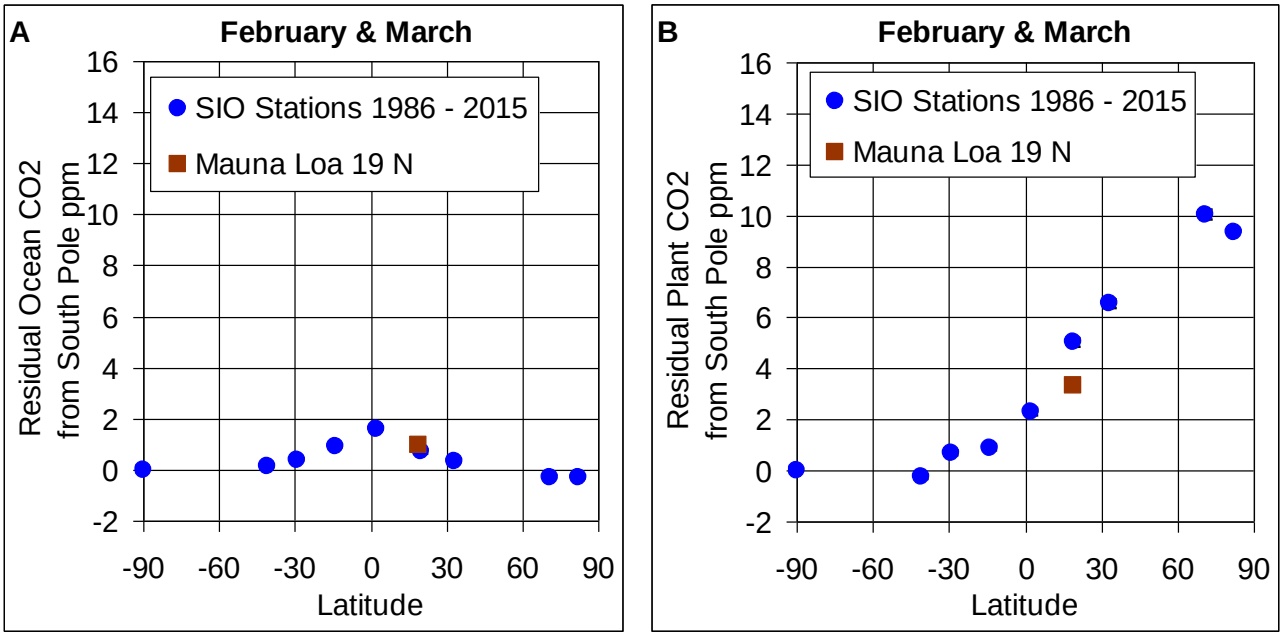

Figure 6. February to March latitude variations of CO2 source components less the year average at the South Pole for the a) ocean source and b) plant source.

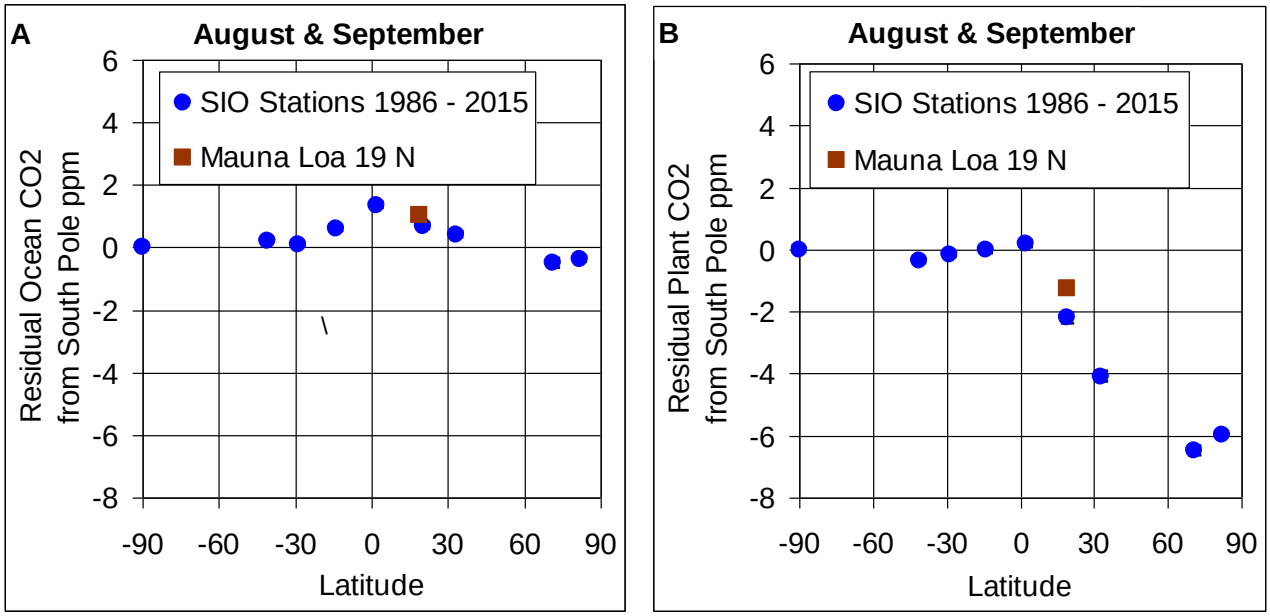

Figure 7. August to September latitude variations of CO2 source components less the value at the South Pole for the a) ocean source and b) plant source.

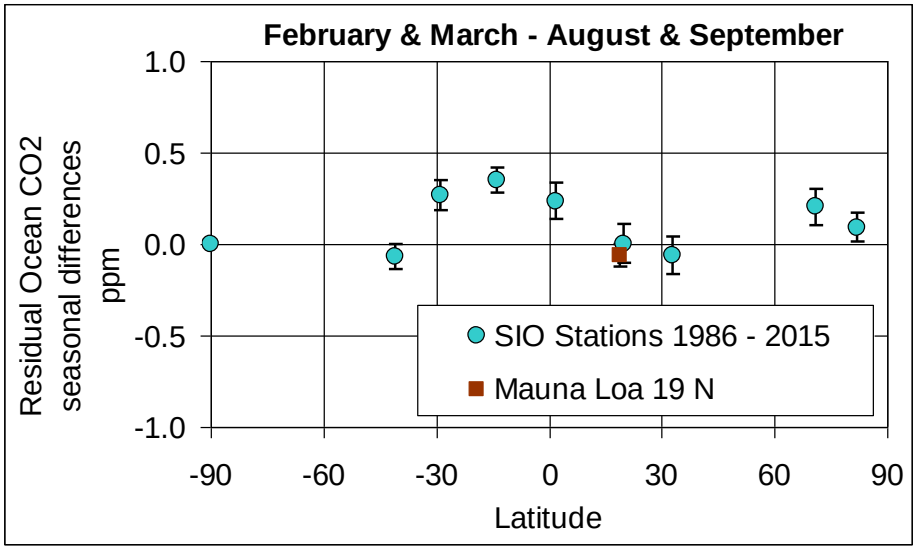

Figure 8. Ocean source seasonal differences for February & March less August & September.

This analysis leads to the conclusion that the seasonal variation of plant source CO2 shows that the ocean source of CO2 is an independent source of atmospheric CO2 and is decoupled from plant source CO2.

5. Sensitivity to assumptions of isotopic composition

The separation into original source components has been made with values for the CO2 ocean component $\delta\,^{13}C = 0$ ‰ and the plant component $\delta\,^{13}C = -26.$ ‰. The sensitivity to this choice has been assessed by varying independently each component $\delta\,^{13}C$ by ± 2 ‰.

The results are shown in Figures 9 and 10 for latitude variations less the source contributions at the South Pole for the period 1986 to 2015.

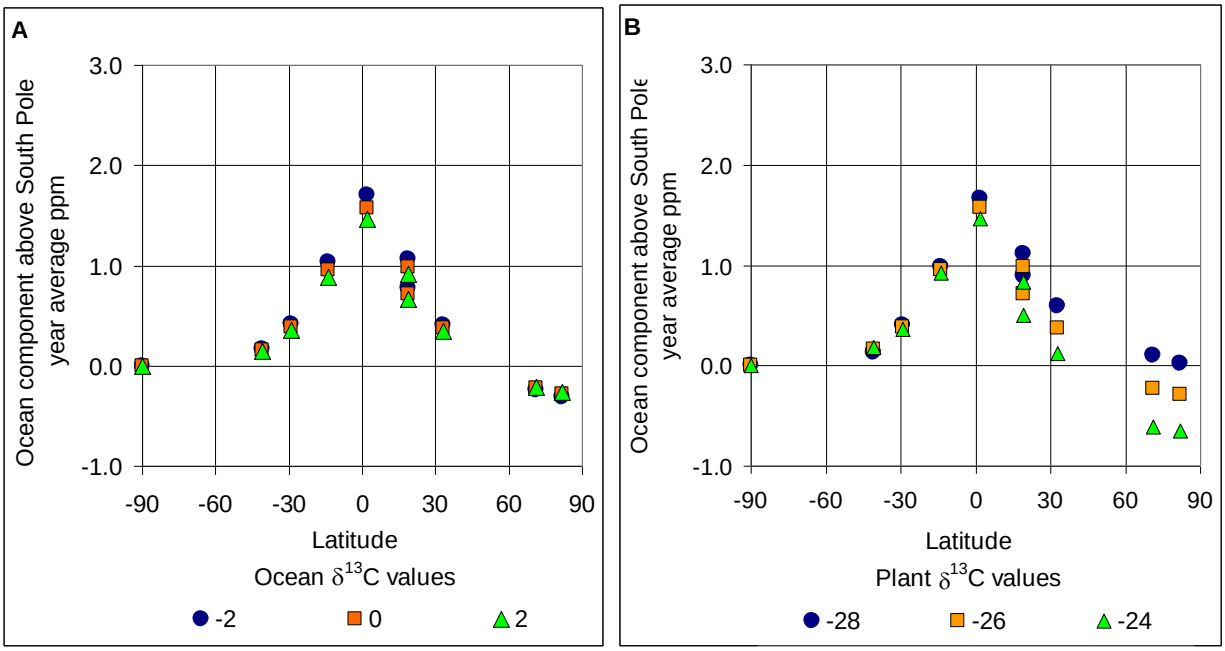

Figure 9. Sensitivity of ocean component CO2 to perturbation of baseline value of $\delta^{13}C$, plotting latitude variations of the ocean components less the year average at the South Pole from 1986 to 2015.for (a) ocean $\delta^{13}C$ value of 0 perturbed by ± 2 and (b) plant $\delta^{13}C$ value of -26 perturbed by ± 2.

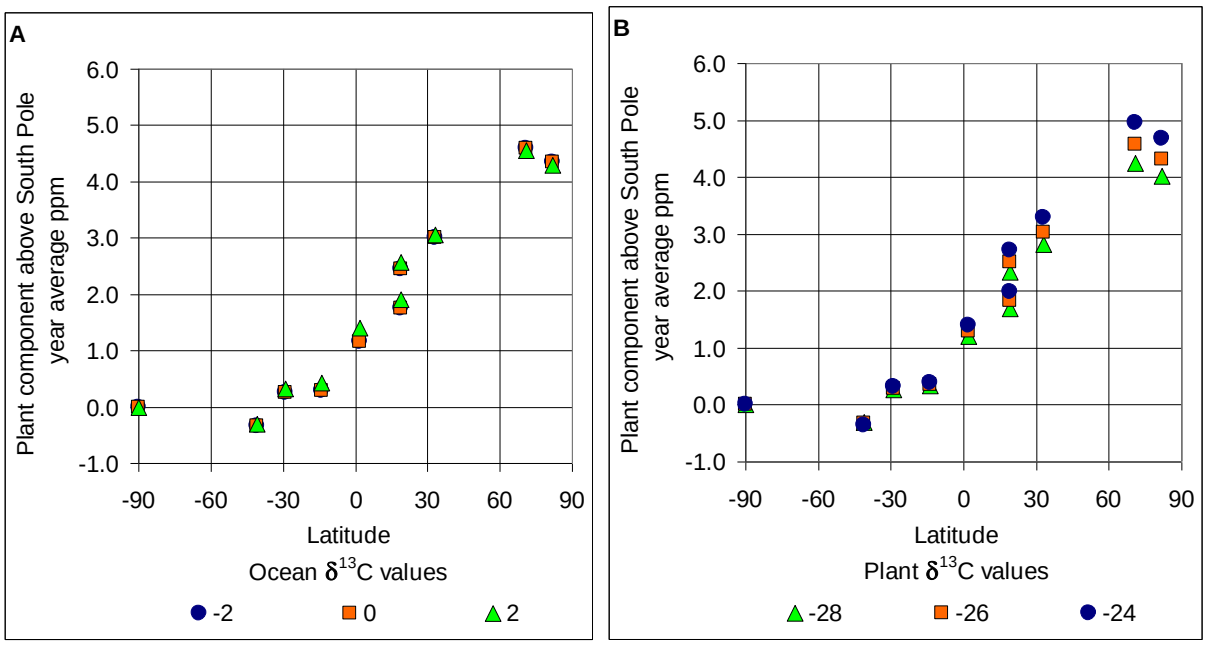

Figure 10. Sensitivity of plant component CO2 to perturbation of baseline value of $\delta^{13}C$, plotting latitude variations of the plant components less the year average at the South Pole from 1986 to 2015. (a) ocean $\delta^{13}C$ value of 0 ‰ perturbed by ± 2. ‰ (b) plant $\delta^{13}C$ value of -26 ‰ perturbed by ± 2. ‰

The shift in values of ocean $\delta^{13}C$ gives a maximum component variation of 0.1 ppm while the shift in values of plant $\delta^{13}C$ gives a maximum component variation of 0.4 ppm.

The variation of isotopic composition of CO2 expressed as variations in $\delta^{13}C$ demonstrates that the patterns of computed changes of ocean and plant components with latitude, are not significantly affected by variations of ± 2 in the baseline values used for $\delta^{13}C$.

6. Annual differences of Ocean and Plant CO2 components

There is more component CO2 variability to be found from the analysis of the annual measured CO2 concentrations and the ocean and plant components. The annual measurements and component values are shown in Figures 11, 12 and 13.

The ocean component (Figure 12) has a significant trend change that has been identified by the use of the Chow Break Test as discussed in reference 3, The break occurs at year 2002±2 and is coincident with a phase change in the Pacific Decadal Oscillation (PDO) [11].

A comparison of the annual plant and ocean component values shows there is more variability in the plant component compared to the ocean component. This can be seen in Figures 12 and 13. The simplest demonstration of variability comes from the standard deviations for the *year on year* changes. The results, given in Table 5, show the ocean components are consistently less variable than the plant component. This should be expected given the inertial properties of the oceans,

Table 5. Station variability.

	Year on year changes: standard deviations in ppm		
Stations	**CO2 concentration**	**Ocean component**	**Plant component**
South Pole 90 S	0.51 ± 0.06	0.34 ± 0.04	0.56± 0.06
Christmas Island 2 N	0.65 ± 0.08	0.47 ± 0.05	0.74 ± 0.09
Mauna Loa 19 N	0.59 ± 0.07	0.33 ± 0.04	0.61± 0.07
Point Barrow 71 N	0.80 ± 0.10	0.28 ± 0.03	0.71 ± 0.08

The annual increases for atmospheric CO2 and components from 1986 to 2015 are given in Table 6. The ocean component is 50% of the annual CO2 concentration increase.

Table 6. Station annual increases from 1986 to 2015.

	Annual increases in ppm		
Stations	**CO2 concentration**	**Ocean component**	**Plant component**
South Pole 90 S	1.79 ± 0.08	0.90 ± 0.05	0.89 ± 0.09
Christmas Island 2 N	1.82 ± 0.11	0.90 ± 0.08	0.92 ± 0.12
Mauna Loa 19 N	1.85 ± 0.10	0.91 ± 0.06	0.94 ± 0.10
Point Barrow 71 N	1.91 ± 0.13	0.91 ± 0.05	0.99 ± 0.12

The complexity of ocean atmosphere interactions and variability may be further analysed by the approach used in reference 3, where residual values of CO2 concentrations were found from strait line least squares fits to the measurements from 1959 to 2007..

The following analysis covers measurements from 1958 to 2018. The residual values are all calculated from a least squares straight line fit to measurements and component values at the South Pole from 1983 to 2018.

Atmospheric CO2 concentrations.

The measurements for the South Pole, Christmas Island, Mauna Loa and Point Barrow are shown in Figure 11 together with the straight line least squares fit to measurements at the South Pole from 1983 to 2018. The residual differences are shown in Figure 14. The trend changes are shown in Figure14 for the Atlantic Multidecadal Oscillation (AMO) for 1966 and 1995 and the Pacific Decadal Oscillation (PDO) in 1977 and 2002 as found in the 2012 analysis (3). The peak in 1989 is coincident with the 1989 Regime Shift (10). A phase change in the AMO occurred in 2012 (14) and this is seen as a trend change in atmospheric CO2 in this extended analysis.

Ocean component values

The ocean component values for the South Pole, Christmas Island, Mauna Loa and Point Barrow are shown in Figure 12 together with the straight-line least squares fit to the ocean component values at the South Pole from 1983 to 2018. The residual differences are shown in Figure 15. There is only one trend change at 2002 +/- 2 at the time of a PDO phase change previously noted in the 2012 analysis (3). The ocean source is centered in the equatorial region of the oceans. There are no AMO trend-changes and the 1989 Regime Shift is not present.

Plant component values

The plant component values for the South Pole, Christmas Island, Mauna Loa and Point Barrow are shown in Figure 13 together with the straight-line least squares fit to the plant component values at the South Pole from 1983 to 2018. The residual differences are shown in Figure 16. The trend changes in Figure16 are for the AMO for 1995 and 2012. The 2012 phase change is from warm to cool. The period from 1995 is a warm period and these variations are seen in phytoplankton variations in productivity.

A study in 2013 (15) looked at the correlation of the AMO with plankton stock variations. The key conclusion is the long-term changes in the standing stock of plankton in the North Atlantic since 1948 mirror the AMO variations. There is then a coincidence of trend changes in the plant CO2 component with phytoplankton variations.

Phytoplankton are at the bottom of the food chain in the oceans. A further study in 2014 (16) showed a correlation of the AMO with fish catches of small pelagic fish. Small pelagic fish, such as herring, sardines, anchovies and sprats feed on plankton in the open oceans.

Productivity falls in AMO cool phases and rises in warm phases presumably due to variations in the sea surface temperature (SST), changes in ocean current circulation and supply of nutrients.

The 1989 Regime Shift (0)was found to be identifiable through the biological time series. This would represent variation in the ocean food chain with phytoplankton at the base with falling SST and changes in ocean current with reduced nutrients and a consequent reduction in their productivity.

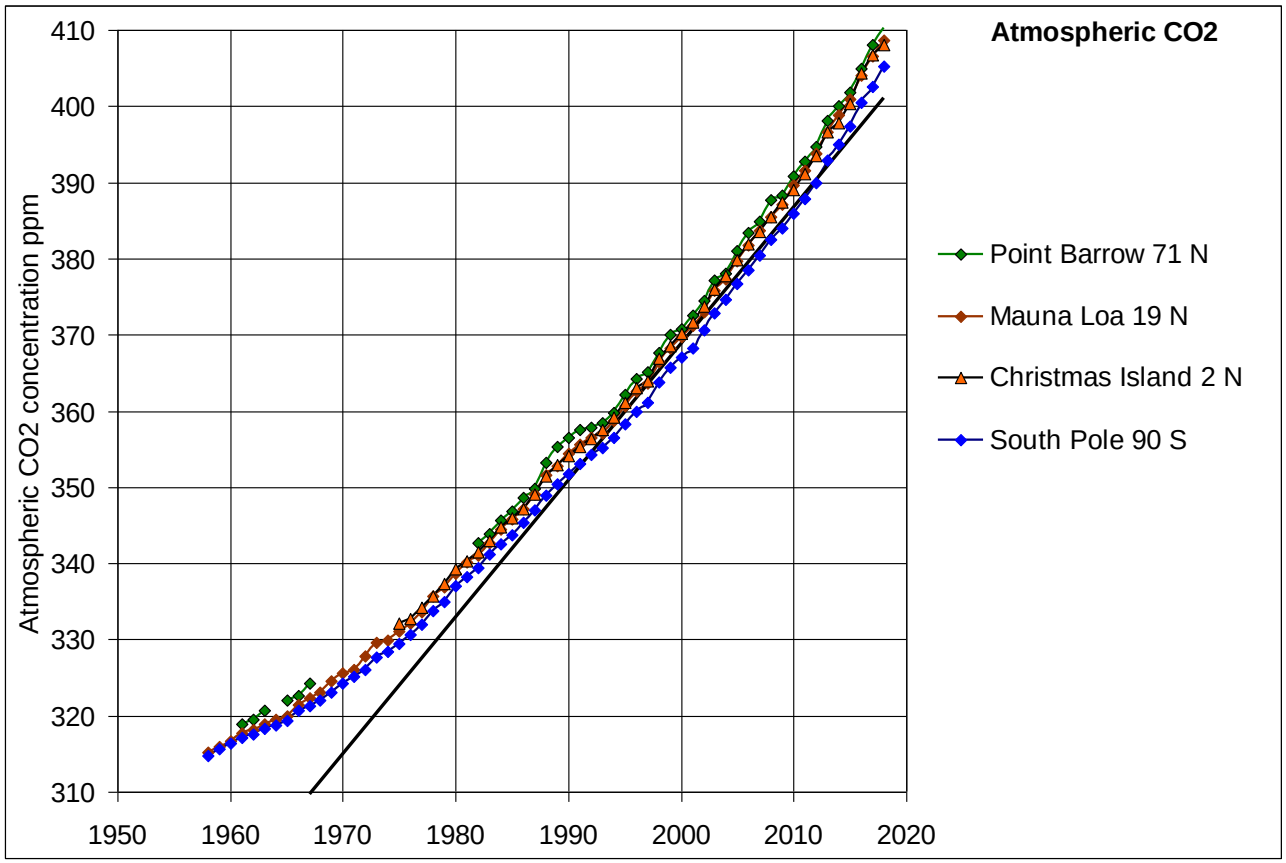

Figure 11. Annual CO2 measurements for the South Pole, Christmas Island, Mauna Loa and Point Barrow Note the straight line fit for the South Pole from 1979 to 2018.

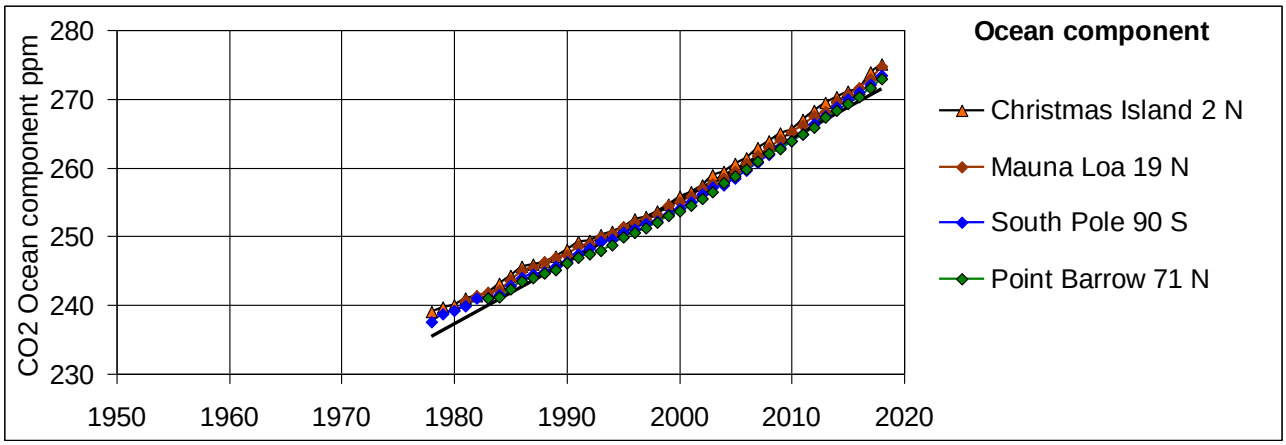

Figure 12. Annual ocean component values for the South Pole, Christmas Island, Mauna Loa and Point Barrow. Note the straight line fit for the South Pole from 1979 to 2018.

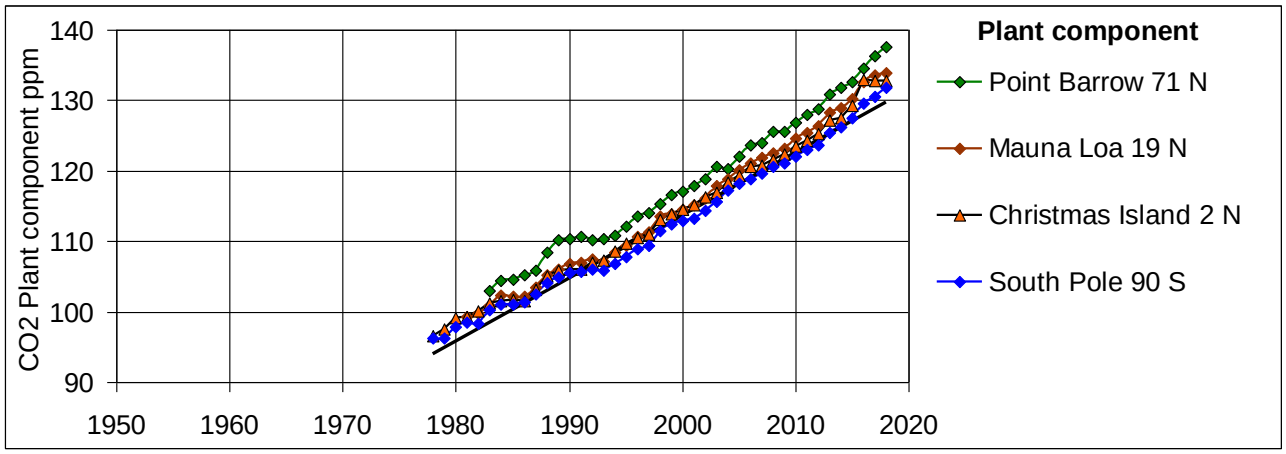

Figure 13. Annual plant component values for the South Pole, Christmas Island, Mauna Loa and Point Barrow. Note the straight line fit for the South Pole from 1979 to 2018

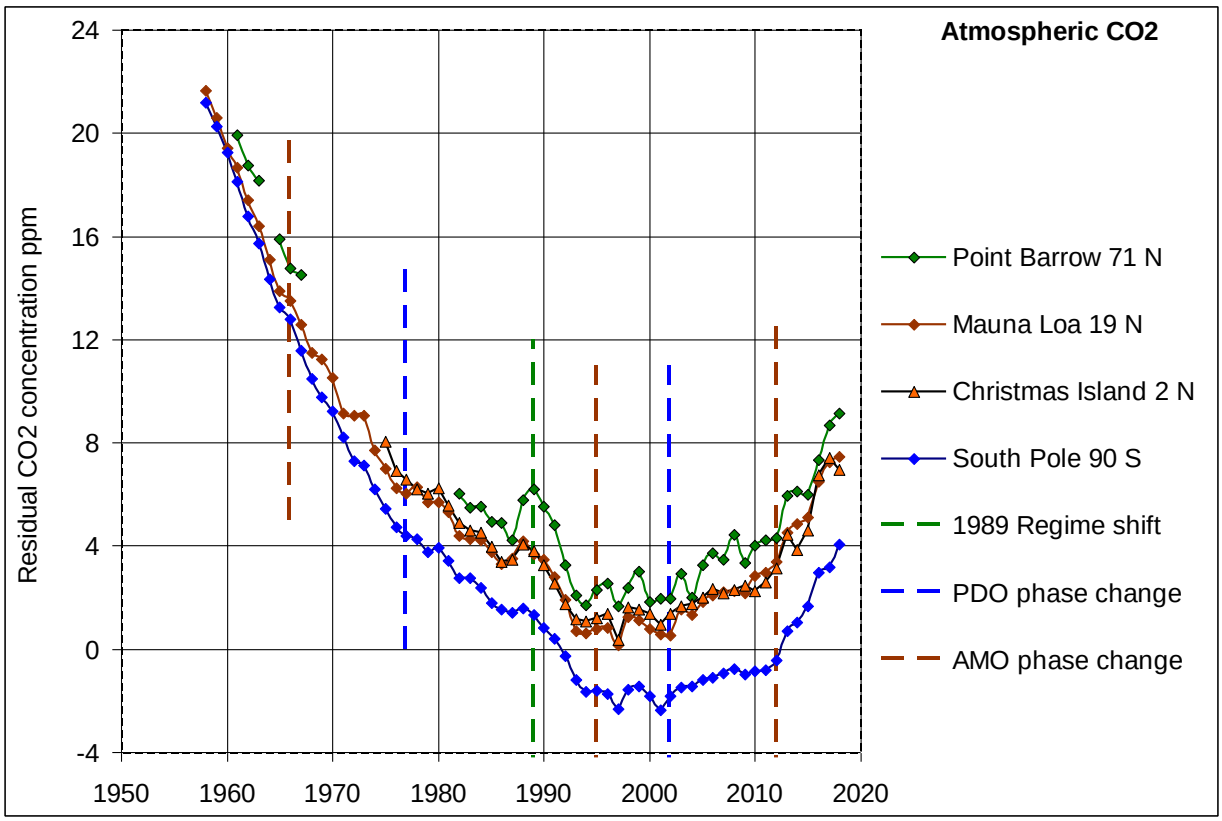

Figure 14. Residual CO2 values for the South Pole, Christmas Island, Mauna Loa and Point Barrow Note the residuals are from the straight line fit to the measurements for the South Pole from 1979 to 2018 .

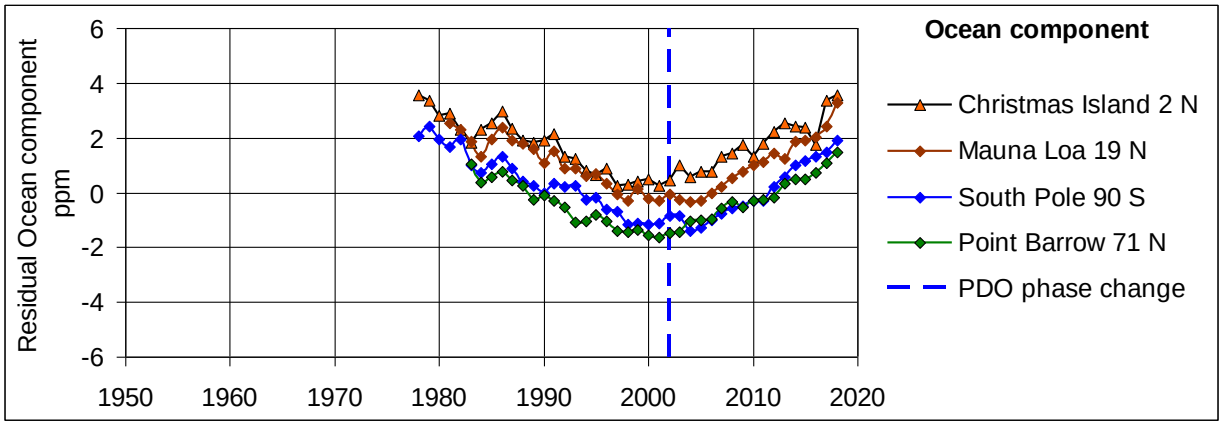

Figure 15. Residual ocean component values for the South Pole, Christmas Island, Mauna Loa and Point Barrow. Note the straight line fit to the ocean component values for the South Pole from 1979 to 2018 ..

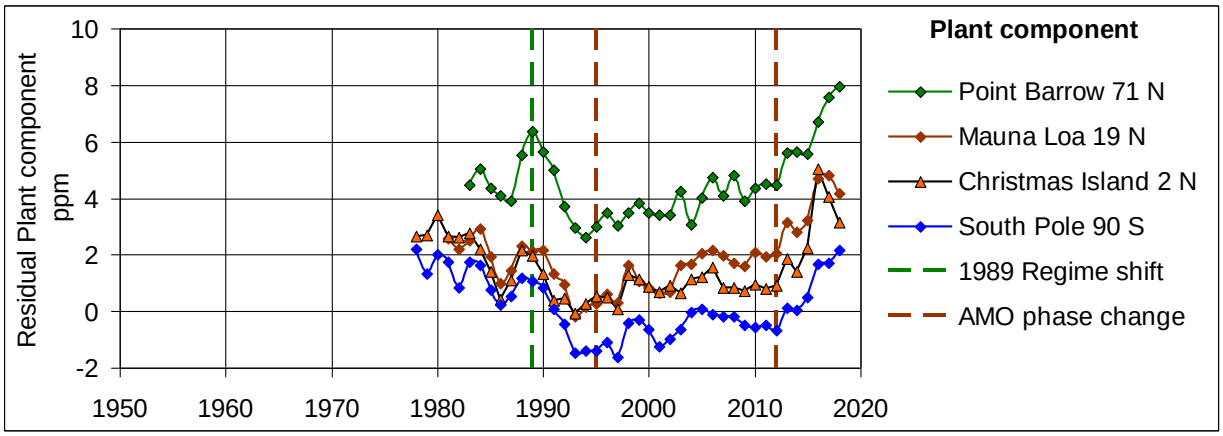

Figure 16. Residual plant component values for the South Pole, Christmas Island, Mauna Loa and Point Barrow. Note the straight line fit to the plant component values for the South Pole from 1979 to 2018

7. Other atmospheric CO2 measurements

While the SIO measurements are the most extensive covering over thirty years, there are two other measurement series. There are extensive CO2 and $\delta^{13}C$ measurements collected by NOAA [12] which run from 1992 to 2014. The CSIRO [13] has measurement that run from 1991 to 2001.

These measurements are consistent with the above analysis results. The Appendix shows the results for 1991 to 2001 where there are overlapping measurements,

8. Discussion and Conclusions

The division of atmospheric CO2 into two original components coming from the ocean and plants including fossil fuel emissions, shows differing behaviour of the components, which indicate that ocean and plant components are independent sources of atmospheric CO2. These results are not significantly affected by perturbation of the assumed baseline values of $\delta^{13}C$ which characterize the isotopic composition of carbon in CO2.

The ocean CO2 component has its maximum value at the equator and we conclude that it is an independent source of atmospheric CO2, as also deduced from its limited year on year variability. We hypothesize that these observations of ocean source CO2 are attributable to upwelling of CO2 rich water transported across the sea floor from the near polar oceans.

The plant CO2 component has more variability than that of the ocean CO2 component and this is attributable to multiple variations in fossil fuel CO2, phytoplankton productivity and forest and peat fires.

In summary this analysis shows

- the ocean and plant components of atmospheric CO2 are independent sources of atmospheric CO2,
- the ocean CO2 component of atmospheric CO2 is in the equatorial region probably associated with deep ocean upwelling
- the plant CO2 component of atmospheric CO2 has a significant variability due to variations in sources of CO2 from fossil fuel emissions and land plants and sinks for CO2 such as phytoplankton and
- approximately 50% of the annual increase in atmospheric CO2 comes from the oceans.

Appendix

Table A1. SIO, CSIRO and NOAA Ocean and Plant Component CO2 Residual Total CO2 and residual Plant and Ocean components from South Pole values

		Lat-itude	Long-itude	Eleva-tion	Years	Residuals 1991 to 2001		
						Total	**Plant**	**Ocean**
SIO	**Alert**	82	-63	210	1986 - 2018	3.63	4.07	-0.44
SIO	**Point Barrow**	71	-157	11	1983 - 2018	3.76	4.36	-0.61
SIO	**La Jolla**	33	-117	14	1979 - 2018	2.92	2.88	0.04
SIO	**Kumukahi**	19	-155	3	1981 - 2018	2.88	2.44	0.44
SIO	**Mauna Loa**	19	-156	3397	1981 - 2018	2.48	1.59	0.89
SIO	**Christmas Island**	2	-157	0	1978 - 2018	2.77	1.46	1.30
SIO	**American Samoa**	-14	-171	42	1985 - 2018	1.21	0.35	0.86
SIO	**Kermadec Island**	-29	-178	2	1985 - 2015	0.54	0.26	0.29
SIO	**Baring Head**	-41	175	80	1986 - 2018	-0.22	-0.24	0.03
SIO	**South Pole**	-90		2810	1978 - 2018	0	0	0
NOAA	**Alert**	82	-63	185	1993 - 2013	3.60	4.02	-0.42
NOAA	**Point Barrow**	71	-157	11	1993 - 2012	4.02	4.58	-0.56
NOAA	**Station M Norway**	66	2	0	1994 - 2009	3.30	3.79	-0.49
NOAA	**Iceland**	63	-20	118	1993 - 2013	2.89	3.37	-0.48
NOAA	**Cold Bay**	55	-163	21	1993 - 2011	3.35	3.75	-0.40
NOAA	**Shemya Island**	53	174	23	1993 - 2012	3.48	3.83	-0.35
NOAA	**Mace Head**	53	-10	5	1994 - 2013	2.98	3.09	-0.11

NOAA	**Cape Meares**	44	-124	30	1992 - 1997	4.22	4.29	-0.07
NOAA	**Mauna Loa**	19	-156	3397	1991 - 2014	2.63	1.78	0.84
NOAA	**Guam**	13	145	0	1992 - 2014	2.56	1.45	1.11
NOAA	**Christmas Island**	2	-157	0	1992 - 2014	2.93	1.99	0.93
NOAA	**Seychelles**	-5	56	2	1991 - 2013	2.91	0.78	2.13
NOAA	**Ascension Island**	-8	-14	85	1992 - 2014	1.04	0.13	0.91
NOAA	**Crozet Islands**	-46	52	197	1995 - 2014	-0.17	0.07	-0.24
NOAA	**South Pole**	-90		2810	1994 - 2018	0	0	0
CSIRO	**Alert**	82	-63	12	1991 - 2001	3.62	3.90	-0.29
CSIRO	**Shetland**	60	-10	30	1994 - 2001	2.58	2.85	-0.27
CSIRO	**Estevan Point**	49	-126	39	1994 - 2001	3.46	3.34	0.12
CSIRO	**Mauna Loa**	19	-156	3397	1992 - 2001	2.49	1.56	0.93
CSIRO	**Cape Ferguson**	-19	147	2	1992 - 2001	0.91	0.06	0.84
CSIRO	**Cape Grim**	-41	145	94	1992 - 2001	-0.01	-0.09	0.08
CSIRO	**Macquarie Island**	-55	159	12	1991 - 2001	-0.17	-0.09	-0.09
CSIRO	**Mawson**	-67	63	32	1991 - 2001	-0.10	0.04	-0.13
CSIRO	**South Pole**	-90		2810	1991 - 2001	0	0	0

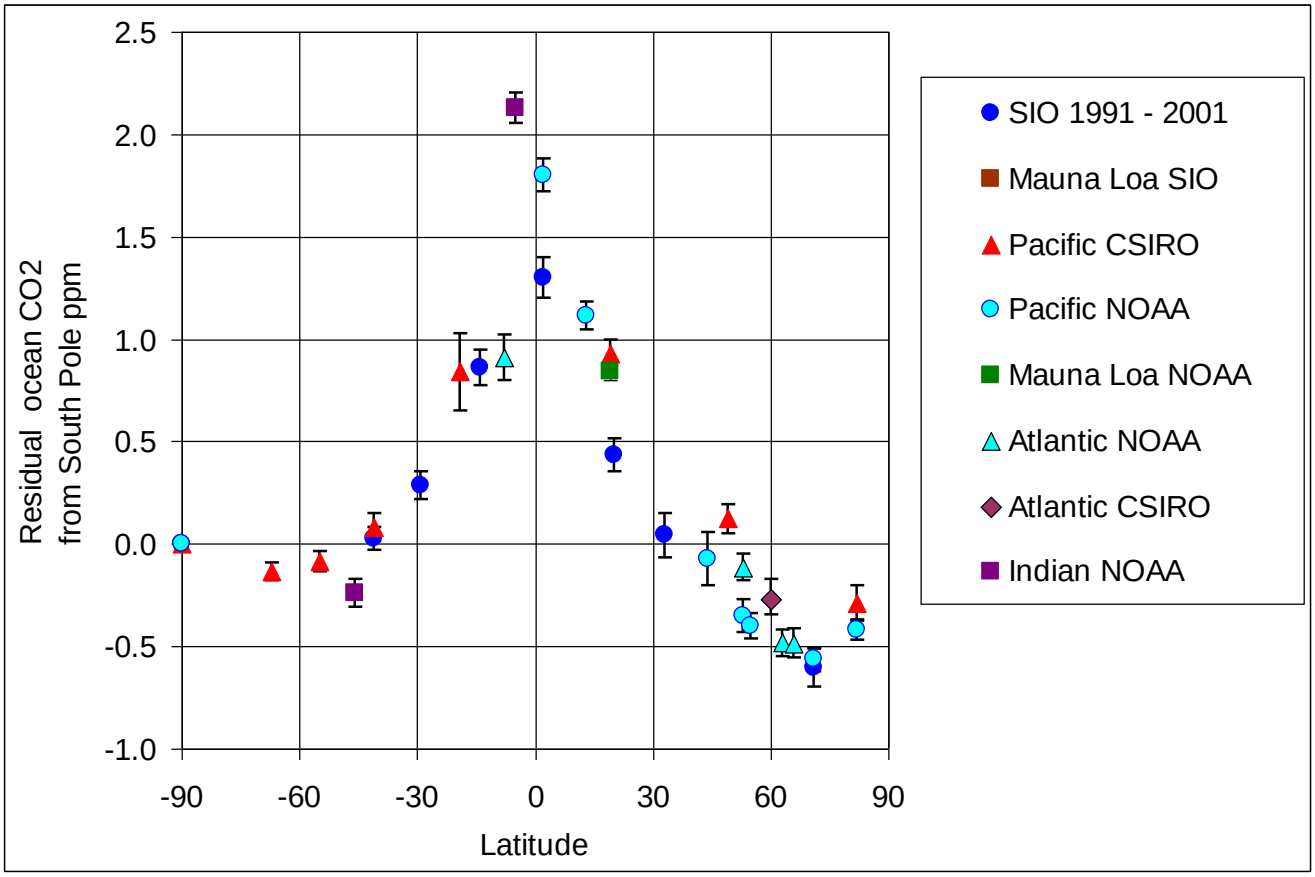

Figure A1. Latitude variations of ocean CO2 source components less the value at the South Pole from SIO, CSIRO and NOAA data for years 1991 to 2001 where there are complete overlapping measurements.

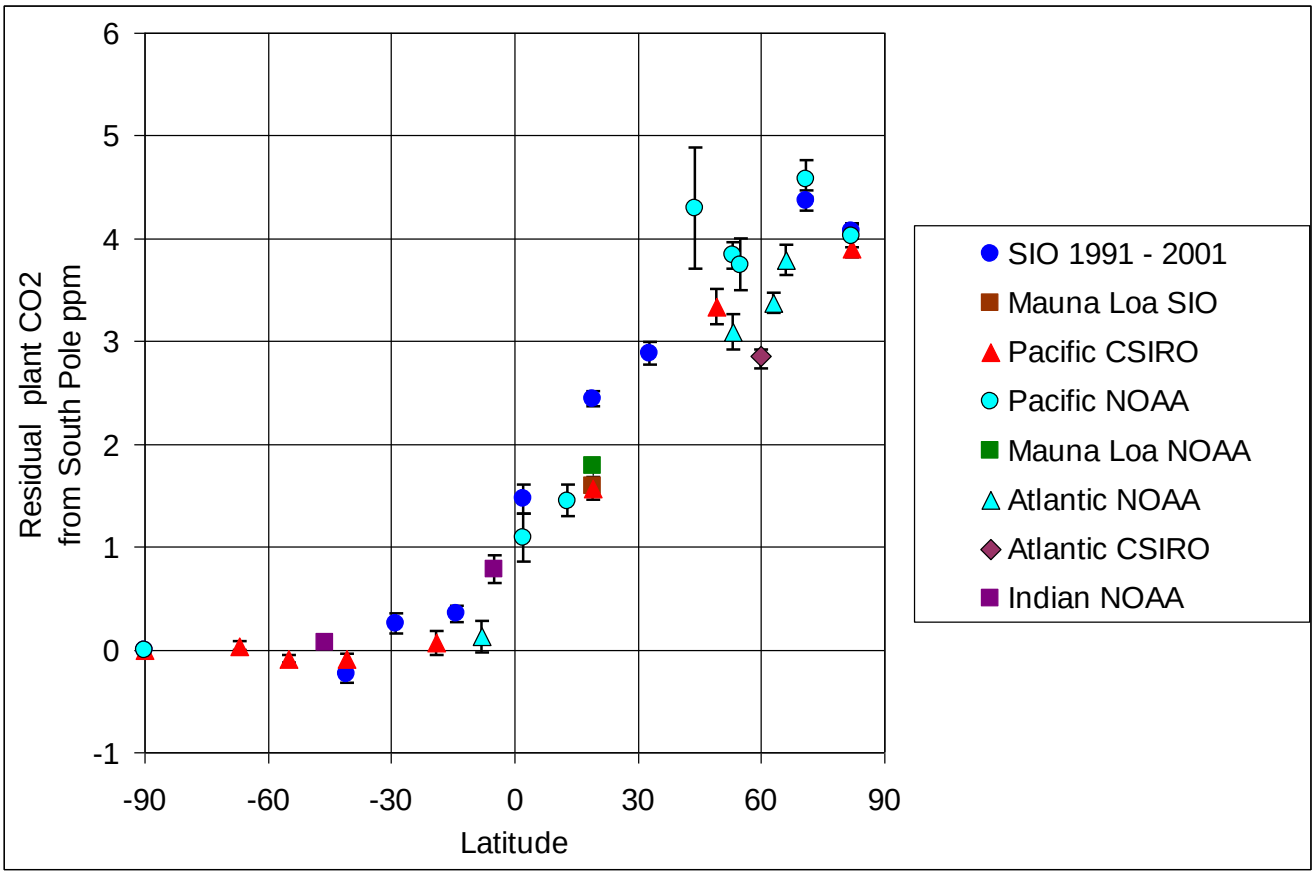

Figure A2. Latitude variations of plant CO2 source components less the value at the South Pole from SIO, CSIRO and NOAA data for years 1991 to 2001 where there are complete overlapping measurements.

References

1. IPCC Fifth Assessment Report Chapter 6 Carbon and Other Biogeochemical Cycles pp 465-571.

2. C. D. Keeling, S. C. Piper, R. B. Bacastow, M. Wahlen, T. P. Whorf, M. Heimann, and H. A. Meijer, Atmospheric CO2 and 13CO2 exchange with the terrestrial biosphere and oceans from 1978 to 2000: observations and carbon cycle implications, pages 83-113, in A History of Atmospheric CO2 and its effects on Plants, Animals and Ecosystems", editors, Etheringer, J.R., T. E. Cerling, M. D. Dearing, Springer Verlag, New York, 2005

3. Quirk, T., 2012, Did the Global Temperature Trend Change at the End of the 1990s? Asia-Pacific J. Atmos. Sci. **2012**, *48(4)*, 339-344, doi:10.1007/s13143-012-0032-4.

4. Kroopnick P. M. The distribution of ^{13}C of ΣCO 2 in the world oceans, Deep-Sea Research **1985**, *32*(1), 57-84.

5. Lynch-Stieglitz J.; Stocker T F.; Broecker W.S.; Fairbanks R.G. The influence of air-sea exchange on the isotopic composition of oceanic carbon: Observations. **1995**, ?????

6. Siegenthaler, U.; Heimann, M.; Oeschger, H. ^{14}C variations caused by changes in the global carbon cycle. Radiocarbon **1980,** *22(2)*, 177-191.

7. O'Leary M. Carbon Isotopes in Photosynthesis Fractionation techniques may reveal new aspects of carbon dynamics in plants, BioScience **1988**, *38(5)*, 328-336.

8. Goericke R.; Fry B. 1994 Variations of marine plankton δ 13C with latitude, temperature, and dissolved CO2 in the world ocean. Global Biochemical Cycles **1994**, *8(1)*, 85-90.

9. Warwick, P.D.; Ruppert, L.F. 2016, Carbon and oxygen isotopic composition of coal and carbon dioxide derived from laboratory coal combustion: A preliminary study. International Journal of Coal Geology **2016**, *166*, 128–135.

10. Hare S.R.; Mantua N.J.:2000, Empirical evidence for North Pacific regime shifts in 1977 and 1989. Progress in Oceanography **2000**, *47*, 103–145.

11. Newman, M., M. A. Alexander, T. R. Ault, K. M. Cobb, C. Deser, E. Di Lorenzo, N. J. Mantua, A. J. Miller, S. Minobe, H. Nakamura, N. Schneider, D. J. Vimont, A. S. Phillips, J. D. Scott, and C. A. Smith, 2016: The Pacific Decadal Oscillation, Revisited. *J. Clim.*, DOI: 10.1175/JCLI-D-15-0508.1

12. Trends: A Compendium of Data on Global Change, Carbon Dioxide Information Analysis Center, Oak Ridge National Laboratory, U.S. Department of Energy, Oak Ridge, TN, U.S.A.,

13. Steele, L.P.; Krummel, P.B.; Langenfelds, R. L. Atmospheric CO_2 concentrations from sites in the CSIRO Atmospheric Research GASLAB air sampling network (August 2007 version). In Trends: A Compendium of Data on Global Change, Carbon Dioxide Information Analysis Center, Oak Ridge National Laboratory, U.S. Department of Energy, Oak Ridge, TN, U.S.A.

14. Frajka-Williams E., Beaulieu C. & Duchez A, Emerging negative Atlantic Multidecadal Oscillation index in spite of warm subtropics. 2017 Scientific Reports | 7: 11224 | DOI:10.1038/s41598-017-11046-x

15. Edwards M, Beaugrand G, Helaoue¨ t P, Alheit J, Coombs S (2013) Marine Ecosystem Response to the Atlantic Multidecadal Oscillation. PLoS ONE 8(2): e57212. doi:10.1371/journal.pone.0057212

16. Jürgen Alheitet al. Atlantic Multidecadal Oscillation (AMO) modulates dynamics of small pelagic fishes and ecosystem regime shifts in the eastern North and Central Atlantic. Journal of Marine Systems 133 (2014) 88–102